Optimization of Incident EC Wave Polarization in Real-Time Polarization Scan Experiments on LHD*)

Toru I. TSUJIMURA[1)], Yoshinori MIZUNO[1)], Ryohei MAKINO[1)], Shin KUBO[1)], Hiroe IGAMI[1)], Takashi SHIMOZUMA[1)], Yasuo YOSHIMURA[1)], Hiromi TAKAHASHI[1,2)], Hiroshi KASAHARA[1,2)], Sakuji KOBAYASHI[1)], Satoshi ITO[1)], Kota OKADA[1)], Takashi MUTOH[1,2)] and the LHD Experiment Group[1)]

[1)]*National Institute for Fusion Science, Toki 509-5292, Japan*
[2)]*SOKENDAI (The Graduate University for Advanced Studies), Toki 509-5292, Japan*

(Received 27 November 2015 / Accepted 11 January 2016)

Real-time polarization scan experiments were performed on the Large Helical Device (LHD) to search an optimal incident wave polarization for electron cyclotron resonance heating. The obtained optimal polarization state to maximize the power absorption to the LHD plasma is compared with the ray-tracing code that includes mode content analyses, which indicates that the calculated results are generally in good agreement with the experimental results. The analyses show that optimal coupling to plasma waves requires a fine adjustment for an incident wave polarization even for perpendicular injection due to the finite density profile and the magnetic shear at the peripheral region.

Keywords: electron cyclotron resonance heating, incident wave polarization, ray-tracing code, mode content analysis, large helical device

DOI: 10.1585/pfr.11.2402016

1. Introduction

A high central electron temperature with an electron internal transport barrier by use of a highly-efficient electron cyclotron resonance heating (ECRH) system is required for steady plasma discharges [1–3]. The operation scenario of the ECRH injection system optimally preset before a discharge can result in a high performance plasma [4]. In addition, feedback control of the ECRH injection system set to an optimal target in real time can create a desired power deposition and reduce the stray radiation in the vessel during a long-pulse discharge [5].

The ray-tracing code *LHDGauss* has been recently upgraded by integration with three-dimensional (3D) equilibrium mapping in ECRH experiments on the Large Helical Device (LHD) [6–8]. The new rapid post-processing procedure enabled adjustments of the ECRH injection settings for the desired deposition profile on a shot-by-shot basis and contributed to an extension of the high-temperature regime in the LHD [6]. Another new feature of *LHDGauss* is that mode purity, which is the ratio between the ordinary (O) mode and the extraordinary (X) mode, can be obtained by solving the 1D full-wave equation along the direction from the injection antenna to the absorption target point. Higher absorption rate of EC waves into LHD plasmas can be expected by optimizing not only the injection direction but also the incident wave polarization of the EC waves with the help of *LHDGauss*, so that the pure O or X mode can be excited at the resonance layer. Especially in the LHD, which has the strong magnetic shear and the finite plasma density at the peripheral region, optimizing the injection polarization setting is an important issue in order to reduce the stray radiation level in the vessel [9, 10].

A recent improvement in rotation stages for polarizers to change rapidly the incident wave polarization in the LHD ECRH transmission lines has enabled real-time fast polarization scan experiments. In this paper, results of the recent real-time polarization scan experiments to find an optimal polarization are described along with comparisons with calculation results with *LHDGauss*. Obtained higher absorption rates are also reported. Section 2 describes an experimental setup of the polarizers for real-time polarization experiments. Section 3 describes results of real-time polarization scan experiments. Section 4 describes discussion on the relation between incident wave polarization and the peripheral region. Section 5 summarizes this paper.

2. Experimental Setup of Polarizers

Each polarizer is mounted on each rotating stage that enables the maximum rotation speed of 180°/s, although the speed is normally restricted to 100°/s for stable use in conventional fixed-polarization experiments. The polarizers are normally controlled by the transmission unification computer. For the purpose of conducting real-time polarization experiments, a feedforward software was spe-

author's e-mail: tsujimura.tohru@nifs.ac.jp

*) This article is based on the presentation at the 25th International Toki Conference (ITC25).

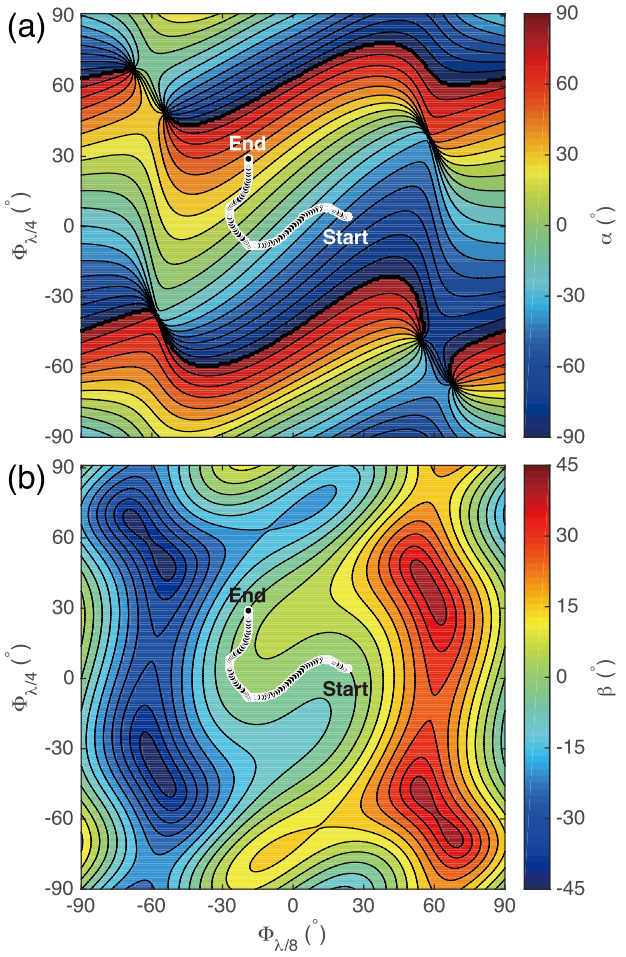

Fig. 1 Time traces of the polarization state (α,β) of the EC wave injected from the 5.5-U port during two plasma discharges #129400 and #129401, which are added on the polarization map of the ECRH #1 (5.5-U, 77 GHz) transmission line. (a) The polarization rotation angle α and (b) the ellipticity β as a function of the angles $\Phi_{\lambda/8}$ and $\Phi_{\lambda/4}$ of the two polarizers installed on the miterbends in the transmission line.

cially developed and it works on the PC, connected to the LHD-ECRH controlling network, instead of on the transmission unification computer. The software confirms that the polarizer reaches the command angle and then orders the polarizer to reach the next command angle. In the real-time polarization scan experiments, the polarization can be changed during a single discharge according to the predefined route on the polarization map for each transmission line. As an example for the real-time polarization scan experiment, an α scan with β fixed was demonstrated, where α and β denote the polarization rotation angle and the ellipticity, respectively. Figure 1 shows time traces of the polarization state (α,β) at the launcher for the EC wave from the 5.5-U port during two plasma discharges. The traces are plotted on the polarization map of the ECRH #1 (5.5-U, 77 GHz) transmission line. $\Phi_{\lambda/8}$ and $\Phi_{\lambda/4}$ denote the rotation angles of the two polarizers, respectively, installed on the miterbends in the transmission line. In the first shot the polarizers rotated from the polarization state of $(\alpha,\beta) \simeq (-45°, 0°)$ to that of $(\alpha,\beta) \simeq (0°, 0°)$, while in the second shot they rotated from the polarization state of $(\alpha,\beta) \simeq (0°, 0°)$ to that of $(\alpha,\beta) \simeq (45°, 0°)$. Each rotation took only 1.2 s although the limited pulse for the high-power 5.5-U EC beam line cost two discharges. The linearly-polarized α scan basically corresponds to switching from X-mode heating to O-mode heating during the discharges for the 5.5-U EC beam line. This operation can be useful for density ramp-up experiments, where the electron density increases over the X2-mode cutoff density during a discharge [11, 12], although only fundamental ECRH is analyzed in this paper.

3. Real-time Polarization Scan Experiments

If the exact boundary between a plasma region and a vacuum region exists, e.g., at the last closed flux surface (LCFS), the millimeter wave injected from the vacuum region couples to a plasma wave at the boundary. The optimal incident wave polarization can be determined with the magnetic field direction at the boundary. However, finite electron density is observed outside of the LCFS of LHD plasmas, where the strong magnetic shear exists, thereby indicating that the exact plasma boundary does not exist due to existence of the plasma/vacuum interface region. In that case, the optimal incident wave polarization needs to be finely searched experimentally or numerically.

The real-time polarization scan experiments were performed under the condition of the electron density approximately fixed and sustained by ICRF (ion cyclotron range of frequency) heating. And the obtained optimal polarization was verified numerically by *LHDGauss*. Figure 2 shows time evolutions of the plasma stored energy, the absorbed power along with the injection power, and the polarization state of the incident EC 77 GHz wave from the 5.5-U port for two discharges with α fixed and scanned, respectively. The modulated ECRH at a frequency of 15 Hz was injected into a low-density plasma with $n_e \sim 1 \times 10^{19}$ m^{-3} in order to estimate the absorbed power experimentally with change of the plasma stored energy from the diamagnetic flux measurement, as described in Ref. [13]. The temporal response of the diamagnetic flux measurement is slow with a time constant of several milliseconds because of uncompensated effects of image currents, so that the time delay effect is taken into account to estimate the absorbed power. As shown in Fig. 2, the two polarizers on the miterbends installed in the transmission line are rotated fast during the injection under control to satisfy that α is scanned rapidly within 1.5 s between 25° and 65° while β is almost fixed at 0°, i.e., α scan. The result indicates that the α scan in real time clearly changes the absorbed power and the power at $\alpha \sim 45°$ is observed to be maximal while $\alpha \sim 25°$ and $\alpha \sim 65°$ exhibit low heating efficiency. Figure 3 shows the calculated ray trajectories of the O mode and the X mode

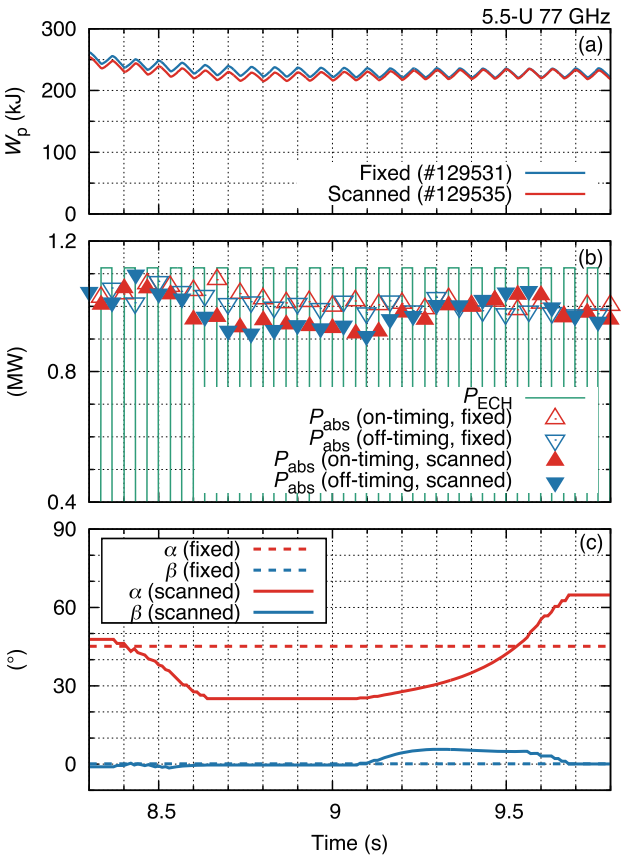

Fig. 2 Time evolutions of (a) plasma stored energy, (b) absorbed power along with injection power, and (c) polarization state (α,β) for the two cases: (i) fixed $(\alpha,\beta) = (45°, 0°)$ and (ii) scanned α with β almost fixed. The absorbed power is evaluated at turn-on and -off timings of the modulated ECRH.

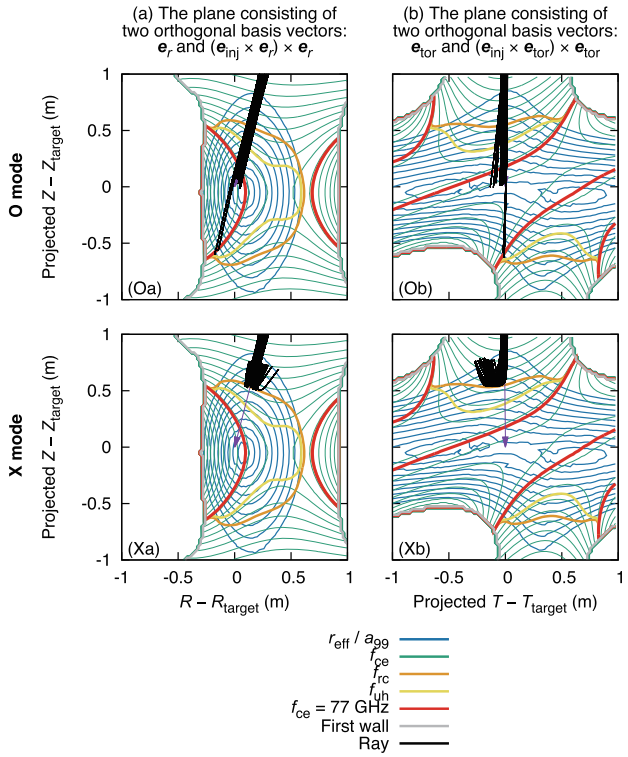

Fig. 3 Calculated ray trajectories of (O) O- and (X) X-mode for the 5.5-U 77 GHz EC beam line under the experimental n_e and T_e profiles along with the 3D equilibrium mapping (LHD shot #129535, $t = 9.54$ s). The projected rays are depicted on the two planes (a) and (b) along with contours of magnetic flux surfaces r_{eff}/a_{99} and electron cyclotron frequencies f_{ce}, lines of the R-wave cutoff frequency f_{rc}, the upper hybrid resonance frequency f_{uh}, and the electron cyclotron resonance frequency f_{ce} for 77 GHz, and the first wall. In the planes, $\mathbf{e}_r$, $\mathbf{e}_{tor}$, and $\mathbf{e}_{inj}$ denote the unit vectors, respectively, in the radial direction at the 5.5-U port center, in the toroidal direction at the 5.5-U port center, and in the direction from the injection antenna center to the target point.

for the 5.5-U 77 GHz EC beam line under the experimental n_e and T_e profiles along with the 3D equilibrium mapping. The magnetic configuration with $B_t = 2.75$ T and $R_{ax} = 3.6$ m assures that the O-mode rays can reach the resonance layer and can be absorbed there while the X-mode rays are reflected at the right-handed (R) wave cutoff layer and cannot be absorbed in a single pass. The change of the absorbed power during the α-scan experiment, as shown in Fig. 2, indicates the change of the O-mode purity.

The optimal polarization obtained experimentally in the scan is confirmed in the mode content analysis implemented in *LHDGauss*. The mode content is determined through solving the 1D full-wave equation along the propagating direction. Figure 4 shows the calculation results. The optimal incident wave polarization is calculated along the inverse propagating direction, i.e., the direction from the R-wave cutoff point to the injection antenna center with the initial polarization set with the pure O-mode polarization in order to obtain the incident polarization state at the injection antenna. The calculated optimal polarization state at $t = 9.54$ s is $(\alpha_{opt},\beta_{opt}) \simeq (47°, 10°)$, which is slightly elliptical. The slight ellipticity contributes to effective power absorption even for nearly perpendicular injection as in the 5.5-U EC beam line. The effect is also confirmed in Fig. 2, where the absorbed power for the polarization state with $(\alpha,\beta) \simeq (45°, 5°)$ (#129535) is higher than that for the polarization state with $(\alpha,\beta) \simeq (45°, 0°)$ (#129531) at $t \simeq 9.54$ s. The absorption rate is improved by approximately 5%. The β effect is considered to be small. However, this effect has to be taken into account when such an MW-class heating device is operated for steady-state experiments.

Figure 5 shows dependence of absorption rate on mode purity. The absorption rate as a function of O-mode purity is plotted for a series of the real-time polarization scan experiments. The experimental O-mode purity is derived by checking orthogonality [14] of an incident wave polarization set experimentally and the optimal incident wave polarization calculated with *LHDGauss* in order to regard the polarization state (α,β) as a physically meaningful parameter such as the O-mode purity in plasma waves.

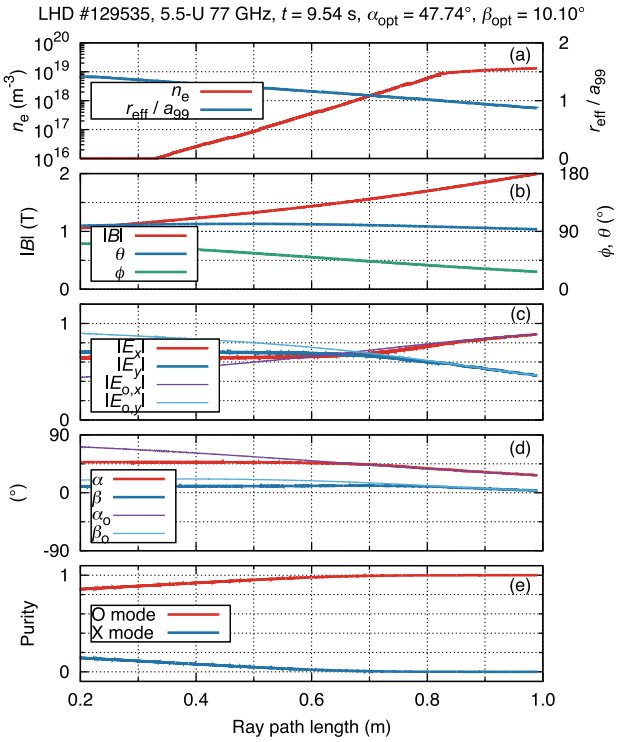

Fig. 4 Calculation results of the 1D full-wave equations along the inverse propagating direction, i.e., the direction from the R-wave cutoff point to the injection antenna center, for the fundamental ECRH operation. (a) the electron density and the normalized minor radius, (b) the strength of the magnetic field, the propagation angle to the magnetic field, and the magnetic shear angle, (c) amplitudes of the electric field components perpendicular to the propagating direction and those of the O-mode electric field components, (d) the polarization states of the electric field and the O-mode electric field, and (e) the O/X-mode purity. The initial polarization is set with the pure O-mode polarization. The resultant optimal incident wave polarization is $(\alpha_{opt},\beta_{opt}) = (47.74°, 10.10°)$. $r_{eff}/a_{99} > 1$ (the outside of the LCFS) shows the extrapolated virtual magnetic flux surfaces.

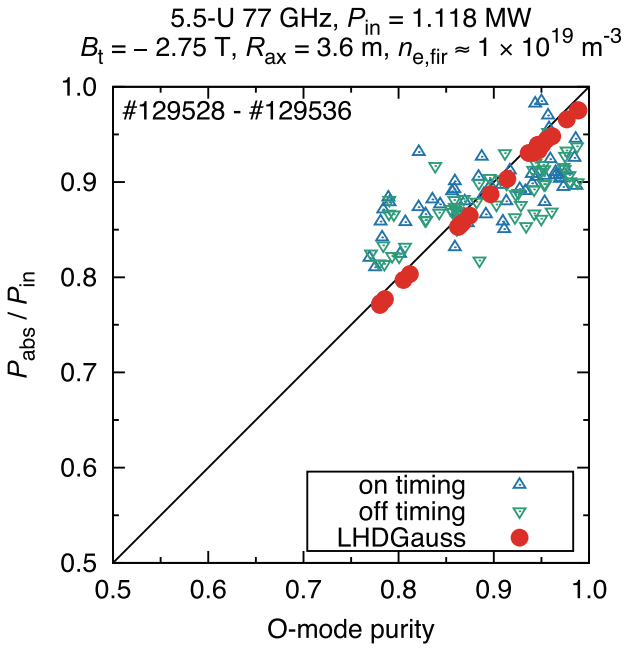

Fig. 5 Absorption rate as a function of O-mode purity.

Figure 5 indicates that the calculated results, which are based on the power deposition profiles of O-mode rays together with the O-mode purity, are generally in good agreement with those evaluated experimentally. Since only the single-pass absorption for the O-mode rays are evaluated in these calculations, the X-mode rays are not absorbed within a single pass. Therefore, when the O-mode purity can be decreased more than that obtained in these experiments, it is expected that the stray radiation due to multi-pass reflection gives rise to a certain amount of power absorption to a plasma. These results suggest that prediction of an optimal polarization with the help of *LHDGauss* is useful when an incident wave polarization has to be finely searched under single-pass absorption guaranteed. Technically speaking, there are still small differences between the experimentally evaluated absorption rate and the calculated one, which remains to be solved. Possible causes to be considered in detail are errors in the experimental evaluation of the absorbed power, errors in the experimental evaluation of the input power, errors in the evaluation of orbit loss in the *LHDGauss* ray-tracing calculation, errors in the evaluation of the model electron density profile in the peripheral region, or the effect of multi-pass reflection.

4. Discussion

It is important to take into account a plasma interface region because optimal coupling to plasma waves is affected by the magnetic shear and the density profile in a peripheral region. According to a previous analytic work [15], the mode coupling effect is not negligible when $\lambda_n > 0.02\tau_s^{0.75}$, where λ_n and τ_s denote scale lengths for the density and the magnetic shear angle, respectively, in equation models at the peripheral region: $n_e(z) = n_c \exp((z - z_c)/\lambda_n)$ and $\phi(z) = \phi_c + 2\pi(z - z_c)/\tau_s$ for $z \le z_c$ along the propagating direction z to the ideal plasma boundary z_c. The criterion describes that the O-mode purity drops less than 90% for $n_c = 1.0 \times 10^{19}\,\mathrm{m}^{-3}$ and 77 GHz. As shown in Fig. 4, the similar situation for the 5.5-U 77 GHz EC wave utilized in the real-time polarization scan experiments locates at around the border of the criterion, i.e., $\lambda_n \simeq 0.02\tau_s^{0.75}$, for $z_c = 0.82$ m (assumed to be the LCFS), $n_c = 8.2 \times 10^{18}\,\mathrm{m}^{-3}$, $\lambda_n = 7.1 \times 10^{-2}$ m, $\phi_c = 0.63$ rad, $|\tau_s| = 5.9$ m, and $0.02|\tau_s|^{0.75} = 7.6 \times 10^{-2}$ m, thereby suggesting that the deviation to excite the pure O mode cannot be negligible when full power absorption is envisaged. Note that the O-mode purity for the analytic work is obtained by comparing the reference optimal polarization state for negligible λ_n and huge τ_s, so that the vacuum condition is satisfied for $z \le z_c$.

5. Summary

The fast real-time polarization scan experiments enable the searching of the optimal incident wave polarization during a short-pulse discharge to increase the ECRH power absorption to the LHD plasma. The polarizers can be moved fast under control on the polarization map. The optimal incident wave polarization obtained in the experiments, which is also expected from the mode content analysis, shows that not only the polarization angle but also the polarization ellipticity need to be optimized even for perpendicular injection when the finite density profile and the magnetic shear at the plasma peripheral region affect the incident wave polarization. Prediction of the optimal incident wave polarization by *LHDGauss* is reliably useful to obtain optimal coupling to plasma waves.

Acknowledgments

This work has been supported by the NIFS LHD project under ULRR701, ULRR804, and ULHH007.

[1] T. Mutoh *et al*., Fusion Sci. Technol. **68**, 216 (2015).
[2] Y. Yoshimura *et al*., Nucl. Fusion, submitted.
[3] H. Igami *et al*., EPJ Web Conf. **87**, 02011 (2015).
[4] H. Takahashi *et al*., Phys. Plasmas **21**, 061506 (2014).
[5] F. Felici *et al*., Nucl. Fusion **50**, 105003 (2010).
[6] T.I. Tsujimura *et al*., Nucl. Fusion **55**, 123019 (2015).
[7] C. Suzuki *et al*., Plasma Phys. Control. Fusion **55**, 014016 (2013).
[8] M. Emoto *et al*., Fusion Eng. Des. **89**, 758 (2014).
[9] T. Notake *et al*., Plasma Phys. Control. Fusion **47**, 531 (2005).
[10] K. Nagasaki *et al*., Phys. Plasmas **6**, 556 (1999).
[11] T. Shimozuma *et al*., Nucl. Fusion **55**, 063035 (2015).
[12] D. Wagner *et al*., Fusion Sci. Technol. **58**, 658 (2010).
[13] R. Makino *et al*., JPS Conf. Proc. **1**, 015034 (2014), Proceedings of the 12th Asia Pacific Physics Conference.
[14] T. Ii *et al*., Rev. Sci. Instrum. **86**, 023502 (2015).
[15] S. Kubo *et al*., 21st Topical Conference on Radiofrequency Power in Plasmas (2015).